Experimental validation of guided wave mode conversion at part-thickness defects in metal plates

L. Li, P. Fromme
Department of Mechanical Engineering, University College London, WC1E 7JE, UK

ABSTRACT

Low frequency guided waves have been used to develop structural health monitoring (SHM) for the early detection of fatigue cracks in metallic aircraft structures. The scattering and mode conversion of guided waves at part-thickness defects was investigated to quantify the sensitivity for defect detection and the potential for the development of a baseline-free SHM methodology employing mode-converted guided waves. Finite Element Analysis (FEA) and experimental validation were conducted to investigate the mode converted scattering from the S_0 to the A_0 Lamb wave mode at part-thickness crack-like defects in an aluminum plate. A piezoelectric (PZT) transducer was experimentally used as a plate edge excitation for the S_0 mode and the out-of-plane displacement was measured using a laser vibrometer. Good agreement between the FEA and experimental results was obtained and the influence of defect depth and length was investigated and quantified.

Keywords: Guided ultrasonic waves, Lamb waves, mode conversion, aluminum plate

1. INTRODUCTION

Guided ultrasonic waves have been studied and used for nondestructive testing (NDT) and structural health monitoring (SHM) of large structures. According to [1], Worlton was one of the first to indicate the potential of guided waves for NDT applications [2, 3]. Guided waves propagating in isotropic plates are called Lamb waves after Horace Lamb [4]. The fundamental symmetric (S_0) and anti-symmetric (A_0) wave modes are two types of Lamb waves at low frequencies (below the cut-off frequency of higher wave modes such as A_1 or S_1 mode) [5]. The FEA method has been widely used for the analysis of guided waves for NDT or SHM. A simple 2D FEA model was developed and used to investigate the scattering of guided waves at a notch in a plate in the early 90s [6, 7] and a notch with depth 8% of thickness of the plate was detectable. The interaction of the S_0 [8] and A_0 [9] modes with a part-thickness notch in a steel plate was studied. Generally, the sensitivity increased as the defect depth increased. The scattering of the A_0 mode at part/through-thickness crack-like defects in an aluminum plate was investigated and the influence of the defect depth, length, and incident wave direction on the detection results were studied [10]. Mode conversion is the phenomenon that part of the energy of one wave mode is transferred to other wave modes as the wave interacts with a part-thickness defect [11]. The mode conversion (S_0-A_0) at a part-thickness hole in a plate was studied [12], but limited research on the scattering and mode conversion at part-thickness crack-like defects in a plate has been conducted. This paper studied the scattering and mode conversion (S_0-A_0) at a part-thickness crack-like defect in a plate. Experimental validation of FEA simulation predictions for variation of defect depth and length was conducted and the sensitivity quantified.

2. EXPERIMENTAL METHODS

An aluminum plate with size 1m x 1m x 5mm was used for the experimental validation (Fig. 1). A piezoelectric (PZT) transducer (Ferroperm Pz27, diameter 5mm, thickness 2mm; brass backing mass, thickness 6mm) was attached using two-component epoxy at the plate edge center to excite the S_0 mode, 500mm away from the plate center where the part-thickness notch was milled. The notch was milled with six different sizes as shown in Table 1. The excitation center frequency was chosen as 100kHz for a frequency-thickness product of 0.5MHzmm below the cut-off frequency of the A_1 Lamb wave mode, where both the S_0 and A_0 mode are reasonably non-dispersive and have significantly different group velocities as shown in Fig. 2 (generated using Disperse software [13]), allowing time separation. A Hanning window was used to modulate the narrowband five cycle toneburst excitation signal. A programmable function generator was used to generate the excitation signal, which was amplified by a voltage amplifier (200Vpp) and applied to the PZT.

Health Monitoring of Structural and Biological Systems XVIII, edited by Zhongqing Su, Kara J. Peters, Fabrizio Ricci, Piervincenzo Rizzo, Proc. of SPIE Vol. 12951, 1295116 · © 2024 SPIE · 0277-786X · doi: 10.1117/12.3012582

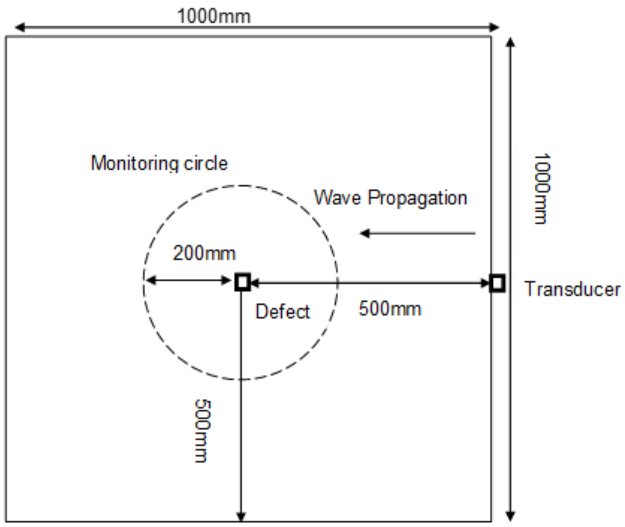

Figure 1. Schematic of plate layout for FEA simulations and experiments, aluminum plate thickness 5 mm.

Table 1. Part-thickness defect size for experimental validation.

Notch length (mm)	Notch depth (mm)
20	1.25
20	2.50
20	3.75
30	3.75
40	3.75
50	3.75

A laser vibrometer was used to measure the out-of-plane displacement velocity on the plate surface at a monitoring circle around the defect (plate center) with 200m radius and 73 measurement points (every 5°). The signals at each measurement point were bandpass filtered (75–125kHz) and averaged (20 averages) using a bandpass filter and digital storage oscilloscope, and then the full time trace data was transferred to a PC for signal analysis.

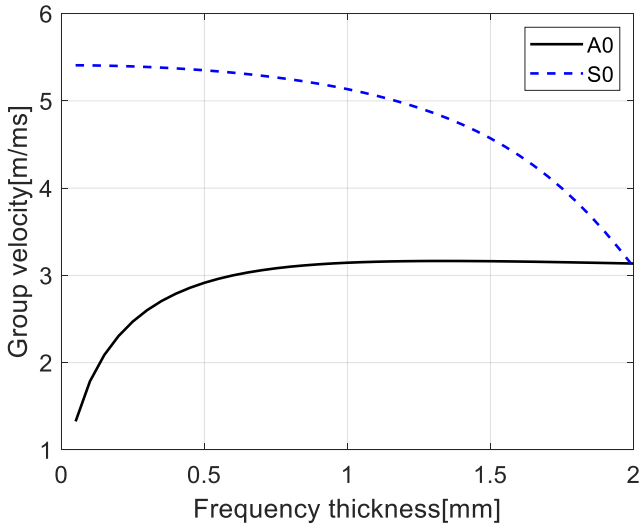

Figure 2. Dispersion diagram for aluminum plate, showing group velocity of the fundamental A_0 and S_0 Lamb wave modes.

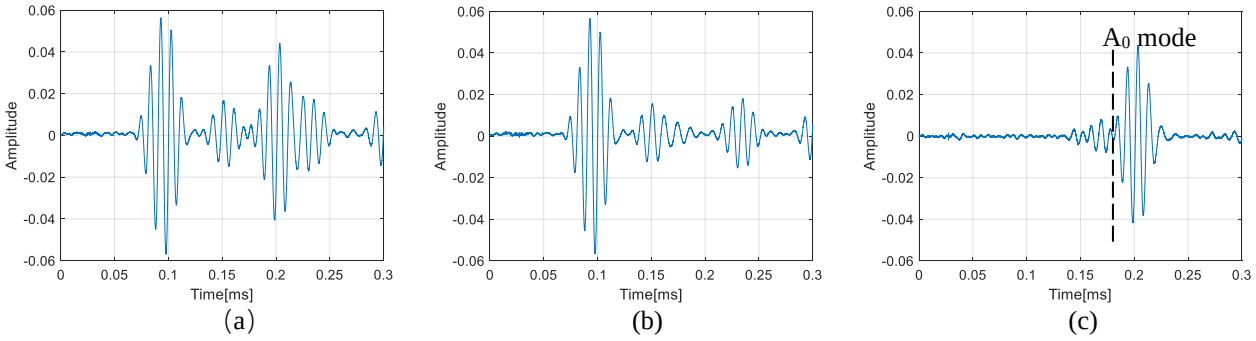

Figure 3. Experimental time trace (baseline subtraction method) for the backward scattered measurement point at a 20mm length, 3.75mm depth defect: (a) measurement with defect, (b) baseline measurement, (c) baseline subtraction; dashed line: cut-off time to separate A_0 mode.

Time gating was applied to separate the scattered A_0 mode, as different modes had different group velocities. The time trace (baseline subtraction) is shown in Fig. 3 and the scattered A_0 mode could be extracted by time gating. Fast Fourier Transform (FFT) was applied to the time trace data to determine the phase and amplitude information at the 100kHz center frequency. Initially the out-of-plane displacement velocity of the incident S_0 mode on the monitoring circle was measured and regarded as the baseline data for the undamaged plate The measured signals were normalized relative to the amplitude of the incident S_0 mode at the undamaged plate center. Unfortunately, the PZT transducer was accidentally knocked off and had to be reattached for the 40mm and 50mm length defect measurements, which negatively influenced the detection results.

3. FEA SIMULATIONS

FEA simulations of the mode conversion (S_0-A_0 mode) at a part-thickness notch were initially reported in a previous contribution [14]. The commercial ABAQUS/Explicit software was used. To match the experiments, the same plate size (1m x 1m x 5mm) was used with material properties of aluminum 6082 (density: 2800kg/m^3, Poisson's ratio: 0.33, Young's modulus: 73GPa). Eight-node linear brick elements with reduced integration (C3D8R) and size 1mm x 1mm x 0.625mm were used. The total simulated time duration was 0.3ms and explicit time integration with a time step of 0.02μs was employed. As the S_0-A_0 mode conversion was studied, an in-plane point force excitation was applied at a plate edge node to simulate the incident S_0 mode excited by the PZT transducer and an additional out-of-plane point force was excited at the same position to simulate the additionally excited A_0 mode in the experiments. The center frequency of the narrowband excitation signal was 100kHz with five cycles, as for the experiments. A crack-like defect was created in the plate center to simulate the experimental notch by removing one row of the brick elements with a notch width of 1mm. Six varying defect sizes were investigated in the FEA simulations, as stated in Table 1. The out-of-plane displacement was recorded at a monitoring circle around the defect center with a 200mm radius on the plate surface and 73 points (every 5°).

4. RESULTS AND DISCUSSION

Time snapshots of the FEA simulations are shown in Fig. 4 to illustrate the incident wave propagation and the scattered mode-converted A_0 mode at the part-thickness defect (size: 30mm length, 3.75mm depth). At 0.1ms (Fig. 4a), the incident S_0 mode and the additionally excited A_0 mode (as in the experiments) can be observed with time separation as the S_0 mode has a faster group velocity than the A_0 mode. At 0.2ms (Fig. 4b), the mode-converted scattered A_0 mode at the defect can be seen in the forward and backward directions. However, the edge reflection of the incident S_0 mode and the additionally incident A_0 mode disturbed the detection results, requiring baseline subtraction to obtain and analyze the pure scattering at the defect. Using baseline subtraction, a good agreement of the polar plots showing the scattered, mode-converted amplitude in different directions between FEA and experimental result was obtained.

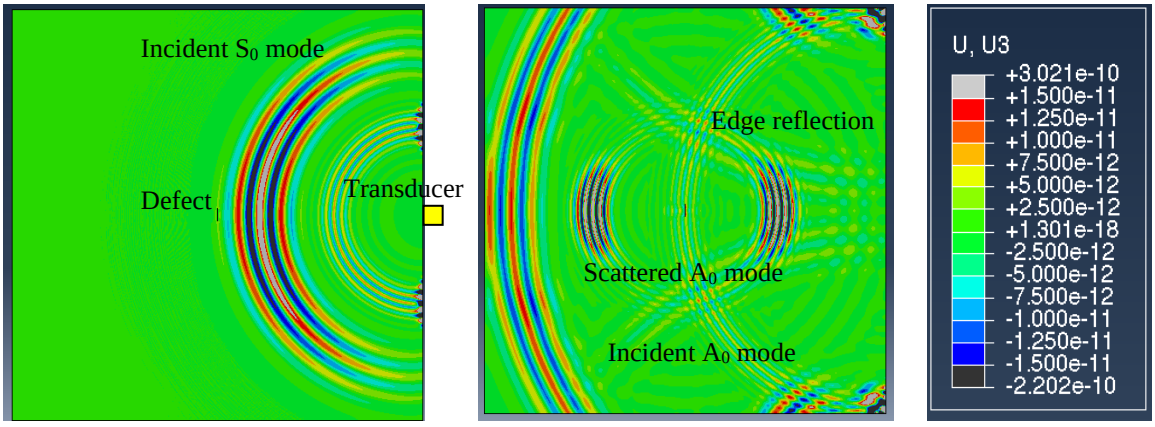

(a) (b)

Figure 4. FEA simulation time snapshots: surface view of the damaged plate (defect size: 30mm length, 3.75mm depth) showing out-of-plane displacement with in-plane point force: (a) 1ms; (b) 2ms.

Generally good agreement of the polar plots between FEA and experimental results can be seen in Fig. 5 and Fig. 6 for variation of the defect depth and length, respectively. Table 2 contains the summary of the relative percentage difference between the FEA and experimental results for each notch size. Backward and forward patterns (two lobes) of the scattered A_0 mode were perpendicular relative to the notch orientation and had similar amplitude (Fig. 5, 6). The sensitivity measured by the normalized amplitude increased as the defect depth or length increased.

Table 2. Percentage difference between FEA predictions and experiments of scattered amplitudes (polar plots) for each notch size.

Defect size	Percentage difference
20mm length, 1.25mm depth	5.0
20mm length, 2.5mm depth	1.2
20mm length, 3.75mm depth	0.4
30mm length, 3.75mm depth	1.6
40mm length, 3.75mm depth	3.5
50mm length, 3.75mm depth	3.0

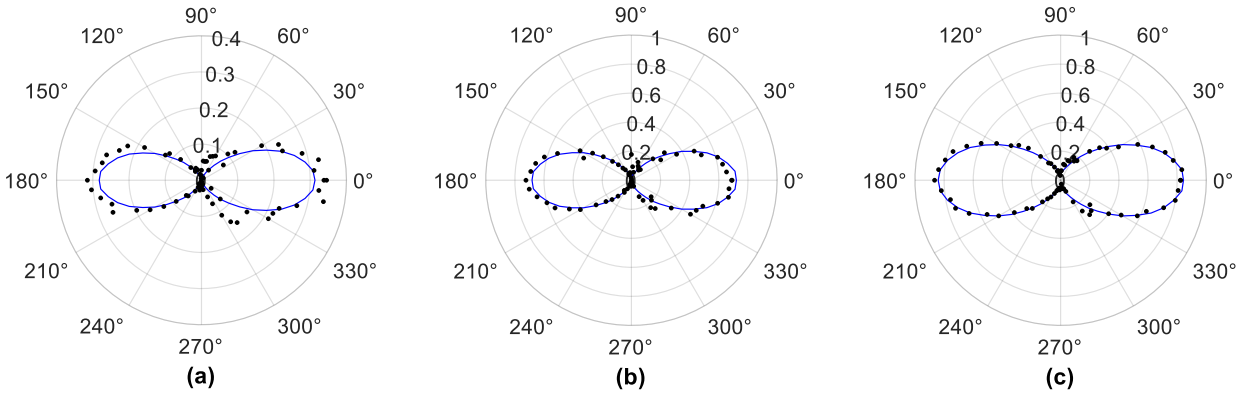

Figure 5. Polar plots of normalized amplitude at defect 20mm length with: (a) 1.25mm depth, (b) 2.5mm depth, (c) 3.75mm depth. FEA simulations: blue solid line; experiments: black dots.

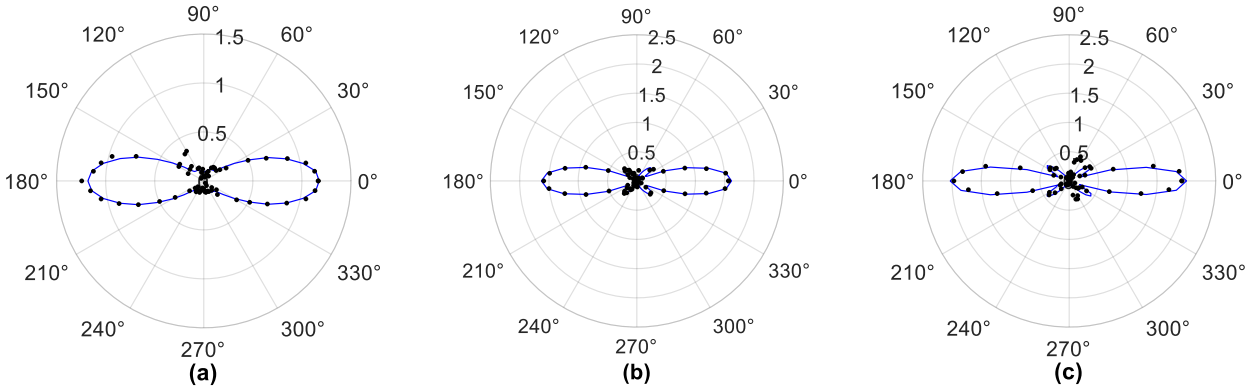

Figure 6. Polar plots of normalized amplitude at defect 3.75mm length with: (a) 30mm length, (b) 40mm length, (c) 50mm length. FEA simulations: blue solid line; experiments: black dots.

For the influence of defect depth on the detection results, an improvement of the agreement was obtained as the defect depth and scattered amplitude increased. The backward and forward scattered lobes had a similar normalized amplitude and the shallow defect (1.25mm depth) gave the largest difference of about 10% between the forward and backward scattered amplitudes of the mode-converted A_0 Lamb wave mode in the 0°-180° direction. The sensitivity (normalized amplitude) increased as the defect depth increased due to the increased scattering and mode conversion energy from the S_0 mode. Although theoretically the highest mode conversion was expected to occur at the half-thickness (2.5mm depth) defect, the highest sensitivity was obtained at the 3/4 (3.75mm) defect depth [14].

For the influence of defect length, due to the knocking off and reattachment of the transducer for the measurements at the 40mm and 50mm depth defects, the agreement was not as good as for the previous measurements at shorter defects (Table 2) but still better than for the shallowest defect depth measurement. The backward and forward patterns had a similar normalized amplitude again with a maximum difference of 1.5% for the 50mm long defect. The normalized amplitude of the scattered A_0 mode increased as the defect length increased. To obtain a better understanding of the scattering and mode conversion at the defect, the influence of the defect size on the detection results could be investigated by FEA simulations as a good agreement and validation was obtained in this contribution.

5. CONCLUSIONS

In this paper, the mode-converted scattering (S_0-A_0 Lamb wave mode) at a part-thickness crack-like defect in an aluminum plate was studied by FEA simulations and experimentally validated. Generally good agreement (less than 5%) between FEA simulations and experimental results was obtained for the polar plot patterns and the normalized amplitude with the variation of the defect size. For a perpendicular incidence of the S_0 mode relative to the defect orientation, the influence of the defect length and depth on the detection results was initially investigated. The backward and forward patterns had a similar normalized amplitude. The highest sensitivity occurred at 3/4-thickness defect depth and increased as the defect length increased, but further investigation is required to incorporate these results for SHM applications of part-thickness fatigue cracks.

REFERENCES

[1] Cawley, P., “Guided waves in long range nondestructive testing and structural health monitoring: Principles, history of applications and prospects,” NDT & E International 142, 103026 (2024). https://doi.org/10.1016/j.ndteint.2023.103026

[2] Worlton, D.C., “Ultrasonic testing with Lamb waves,” United States: N.P. (1956). https://doi.org/10.2172/4356069

[3] Worlton, D.C, “Experimental confirmation of Lamb waves at megacycle frequencies,” Journal of Applied Physics 32(6), 967-971 (1961). https://doi.org/10.1063/1.1736196
[4] Lamb, H., “On waves in an elastic plate,” Proceedings of the Royal Society London A 93, 114–128 (1917). http://doi.org/10.1098/rspa.1917.0008
[5] Rose, J.L., “Ultrasonic Guided Waves in Solid Media,” Cambridge University Press (2014).
[6] Alleyne D.N, “The nondestructive testing of plates using ultrasonic Lamb waves,” London: PhD thesis University of London (Imperial College) (1991).
[7] Alleyne, D.N. and Cawley, P., “The interaction of Lamb waves with defects,” IEEE Transactions on Ultrasonics Ferroelectrics and Frequency Control 39(3), 381-397 (1992). https://doi.org/10.1109/58.143172
[8] Lowe, M.J.S. and Diligent, O., "Low-frequency reflection characteristics of the s(0) Lamb wave from a rectangular notch in a plate," Journal of the Acoustical Society of America 111(1), 64-74 (2002). https://doi.org/10.1121/1.1424866
[9] Lowe, M.J.S., Cawley, P., Kao, J.Y. and Diligent, O., "The low frequency reflection characteristics of the fundamental antisymmetric Lamb wave alpha(0) from a rectangular notch in a plate," Journal of the Acoustical Society of America 112(6), 2612-2622 (2002). https://doi.org/10.1121/1.1512702
[10] Fromme, P., "Guided wave sensitivity prediction for part and through-thickness crack-like defects," Structural Health Monitoring 19(3), 953-963 (2020). https://doi.org/10.1177/1475921719892205
[11] Cho, K., "Estimation of ultrasonic guided wave mode conversion in a plate with thickness variation," IEEE Transactions on Ultrasonics Ferroelectrics and Frequency Control 47(3), 591-603 (2000). https://doi.org/10.1109/58.842046
[12] Cegla, F.B., Rohde, A. and Veidt, M., "Analytical prediction and experimental measurement for mode conversion and scattering of plate waves at non-symmetric circular blind holes in isotropic plates," Wave Motion 45(3), 162-177 (2008). https://doi.org/10.1016/j.wavemoti.2007.05.005
[13] Pavlakovic, B., Lowe, M., Alleyne, D. and Cawley, P., “Disperse: A general purpose program for creating dispersion curves,” In: Thompson, D.O., Chimenti, D.E. (eds) Review of Progress in Quantitative Nondestructive Evaluation, 16, 185-192 (1997). https://doi.org/10.1007/978-1-4615-5947-4_24
[14] Li, L. and Fromme, P., “Mode-converted Lamb wave sensitivity prediction for part-thickness crack-like defect,” Proceedings SPIE 12488, 1248821 (2023). https://doi.org/10.1117/12.2657951